PHYSICAL REVIEW C

NUCLEAR PHYSICS

THIRD SERIES, VOLUME 34, NUMBER 4 OCTOBER 1986

$M4$ excitations in ^{13}C

R. S. Hicks, R. A. Lindgren,* M. A. Plum,† and G. A. Peterson
University of Massachusetts, Amherst, Massachusetts 01003

Hall Crannell and D. I. Sober
Catholic University of America, Washington, D.C. 20064

H. A. Thiessen
Los Alamos National Laboratory, Los Alamos, New Mexico 87545

D. J. Millener
Brookhaven National Laboratory, Upton, New York 11973
(Received 18 November 1985)

Cross sections for the 9.50, 16.08, and 21.47 MeV $M4$ transitions in ^{13}C have been measured by inelastic electron scattering. Isoscalar and isovector transition amplitudes were deduced by comparison with (π,π') and (p,p') data. In particular, the transition amplitudes obtained for the 9.50 MeV excitation give a remarkably consistent description of all existing measurements. A comparison was made with $M4$ transitions in other carbon isotopes, ^{12}C and ^{14}C. In each case, detailed shell model calculations accurately predict the energies, relative strengths, and isospin character of the observed $M4$ transitions. However, the shell model gives (e,e') $M4$ cross sections that exceed the data by a factor of 2.

I. INTRODUCTION

Inelastic scattering experiments have established the existence of high-multipole, $1\hbar\omega$ magnetic transitions to "stretched" spin states, i.e., one-particle–one-hole states in which the highest spin orbitals of adjacent oscillator shells are coupled to the maximum possible angular momentum. The relative simplicity of these transitions is assumed because other configurations of the same spin and parity lie at least two oscillator shells higher in excitation energy. Thus the interpretation of data on stretched states is rather model-independent, and one can hope to gain clear insights into properties such as subshell occupation numbers and Pauli blocking effects, possible quenching of nucleon magnetic moments, and the radial size of valence orbitals. Furthermore, since one-body excitation of these states involves only the spin-flip transition density,[1] the transitions have proven valuable for the direct comparison of reactions utilizing various probes.

Almost all of the available information on stretched magnetic transitions pertains to even-A nuclei. Although the same transition should exist in odd-A nuclei, it is expected that the cross sections will be fragmented by the presence of the unpaired valence nucleon. Thus far, the most compelling evidence for observable stretched magnetic transitions in an odd-A nucleus is perhaps found in ^{13}C, where stretched $M4$ transitions, corresponding to the $(d_{5/2},p_{3/2}^{-1})_{M4}$ configuration, have been indicated in inelastic pion[2–4] and proton[5–7] scattering, as well as in photoproduction[8] and reactions initiated by ^3He and ^4He projectiles.[9,10] The present paper reports the observation of these transitions by means of inelastic electron scattering. It will be shown that the results obtained using various probes complement each other, and provide a rather detailed picture of the properties of $M4$ excitations in ^{13}C. A comparison of the experimental results with shell model calculations will demonstrate that a rather comprehensive theoretical understanding exists for these high-multipole transitions in odd-A nuclei.

II. EXPERIMENTAL PROCEDURES

The experiment utilized the electron scattering facility[11] of the Bates Linear Electron Accelerator in Middleton, Massachusetts. Measurements were made at laboratory scattering angles of 45°, 90°, 160°, and 180° for incident electron energies ranging from 78 to 338 MeV. The data extend over a three-momentum transfer range of

TABLE I. Shell model results for $M4$ transitions in ^{13}C, including estimates of (e,e') form factors (in arbitrary units) and (π,π') cross sections (in μb/sr).

E_x (MeV)	$J_f^+;T$	Z_0	Z_1	F^2	σ^-	σ^+
7.57	$\frac{7}{2};\frac{1}{2}$	−0.0711	−0.1095	0.9	6	0
9.45	$\frac{9}{2};\frac{1}{2}$	0.3423	0.3300	7.1	102	12
12.46	$\frac{7}{2};\frac{1}{2}$	0.1234	0.0461		9	4
14.05	$\frac{7}{2};\frac{1}{2}$	−0.0966	−0.0434			
15.46	$\frac{9}{2};\frac{1}{2}$	0.1099	−0.1060	1.6	1	11
15.90	$\frac{7}{2};\frac{1}{2}$	−0.1929	0.2692	9.3	1	42
16.13	$\frac{7}{2};\frac{1}{2}$	0.1471	0.1241	0.9	17	3
16.80	$\frac{7}{2};\frac{1}{2}$	0.0777	−0.0377			
16.88	$\frac{9}{2};\frac{1}{2}$	0.2055	−0.1512	3.6	7	31
18.57	$\frac{7}{2};\frac{1}{2}$	−0.1252	−0.0391		8	4
18.89	$\frac{9}{2};\frac{1}{2}$	0.0945	−0.1087	1.6	1	9
19.19	$\frac{9}{2};\frac{1}{2}$	−0.1903	0.0155		13	16
19.34	$\frac{7}{2};\frac{1}{2}$	0.2245	0.0228		22	18
19.95	$\frac{7}{2};\frac{1}{2}$	0.0461	0.0070			
19.99	$\frac{9}{2};\frac{1}{2}$	−0.2103	−0.0312		20	15
20.48	$\frac{7}{2};\frac{1}{2}$	0.0490	−0.0453			
20.69	$\frac{7}{2};\frac{3}{2}$		0.1807	3.3		
20.78	$\frac{7}{2};\frac{1}{2}$	0.0944	0.0289			
21.25	$\frac{9}{2};\frac{1}{2}$	0.2354	−0.0120		21	23
21.48	$\frac{9}{2};\frac{3}{2}$		−0.5213	27.2	27	27
21.57	$\frac{7}{2};\frac{1}{2}$	−0.2873	0.0122		31	34
21.78	$\frac{7}{2};\frac{1}{2}$	−0.1492	−0.0870		15	4
21.90	$\frac{7}{2};\frac{1}{2}$	−0.0833	0.0734	0.8		
21.92	$\frac{9}{2};\frac{1}{2}$	0.0666	0.0830			
22.01	$\frac{7}{2};\frac{3}{2}$		−0.3990	15.9	16	16
22.08	$\frac{9}{2};\frac{1}{2}$	−0.2842	0.1125	2.7	21	46
22.72	$\frac{7}{2};\frac{1}{2}$	−0.1460	−0.0549		12	6
22.98	$\frac{7}{2};\frac{1}{2}$	−0.1255	−0.0095			
22.99	$\frac{9}{2};\frac{1}{2}$	−0.2286	−0.0604		27	16
23.43	$\frac{7}{2};\frac{1}{2}$	0.0322	0.0383			
23.77	$\frac{7}{2};\frac{1}{2}$	−0.1952	−0.0176		16	14
23.94	$\frac{7}{2};\frac{3}{2}$		0.0611			
24.51	$\frac{9}{2};\frac{1}{2}$	−0.0862	0.0500			
24.65	$\frac{9}{2};\frac{3}{2}$		0.0711			
26.29	$\frac{7}{2};\frac{3}{2}$		0.1965	3.9		
26.95	$\frac{9}{2};\frac{1}{2}$	0.1213	−0.0122			
27.30	$\frac{7}{2};\frac{3}{2}$		−0.0784			
27.67	$\frac{7}{2};\frac{3}{2}$		−0.0645			
27.93	$\frac{9}{2};\frac{1}{2}$	0.0982	−0.0211			
28.78	$\frac{9}{2};\frac{3}{2}$		0.1585	2.5		

$q=0.5$–3.3 fm^{-1}. Effective target thicknesses of up to 0.20 g cm^{-2} were used with spectrometer acceptance solid angles as large as 3.51 msr. The maximum time-averaged electron current incident on the ^{13}C target was about 40 μA. Further details of the experimental techniques and data analysis procedures can be found in Ref. 12, as can the conventions followed in the definition of the (e,e') form factors. A complete tabulation of the data is available from the Physics Auxiliary Publication Service (PAPS) depository.[13]

III. SHELL MODEL

Details of the shell model procedures can be found elsewhere.[14] In brief, the ^{13}C ground state was derived from Cohen-Kurath (8–16)2BME two-body matrix elements.[15] Even-parity states were calculated in a complete $1\hbar\omega$ space with a slightly modified form of the Millener-Kurath[14] effective interaction. Table I lists results for the states relevant to this work, the $\frac{7}{2}^+$ and $\frac{9}{2}^+$ levels. The isoscalar ($\Delta T=0$) and isovector ($\Delta T=1$) transition amplitudes or one-body density matrix elements[16,17] Z_0 and Z_1 shown in Table I are defined to equal unity for a pure particle-hole excitation of a closed shell nucleus with $J=0$ and $T=0$. These transition amplitudes are related to A_n and A_p, the neutron and proton transition amplitudes of Lee and Kurath,[18] by means of $Z_0=M(A_n+A_p)$ and $Z_1=M(A_n-A_p)$, where

$$M=(2J_f+1)/(2J_i+1)(2\Delta J+1)\sqrt{2}\ .$$

Also given in Table I are estimates of $M4$ excitation strengths for (π,π') and (e,e') reactions. At the peak of the (π,π') $M4$ angular distribution, the differential π^- and π^+ cross sections are given approximately by[18] $\sigma^{\mp}\cong 99(2Z_0\pm Z_1)^2$ (μb/sr). As a measure of the (e,e') form factor magnitude we use $100(Z_1-0.187Z_0)^2$. The same information, apart from slight changes in the shell-model calculations, is given in Fig. 13 of Ref. 18.

The $M4$ strength in ^{13}C is generally found in states having sizable amplitudes for a $d_{5/2}$ particle coupled to core states with large $p_{3/2}$ spectroscopic factors S($p_{3/2}$), namely[19] the lowest $J^\pi=1^+$ and 2^+ levels with $T=0$ and $T=1$. Table II shows the weak-coupling representations for some of the states expected to be strongly excited in (e,e'). The $(2^+;T=0)\otimes d_{5/2}$ strength is concentrated in the first $\frac{7}{2}^+$ and $\frac{9}{2}^+$ levels predicted at 7.57 and 9.45 MeV. Broadly speaking, strength based on the three core levels between 12 and 16 MeV tends to gather near 16 MeV for $T=\frac{1}{2}$ states in ^{13}C, and around 21.5 MeV for $T=\frac{3}{2}$ states. Sum rules[20] for the transition amplitudes

$$\sum_f Z^2=\tfrac{1}{8}\sum_{\text{core}} S(p_{3/2})$$

are simply given by the occupancy of the $p_{3/2}$ orbit independent of ΔT. In $^{12,13,14}C$ the respective occupancies obtained[19] using the Cohen and Kurath wave functions are 0.810, 0.924, and 0.959. The sum rule is easily broken down into contributions for specific J_f, T_f, and ΔT. For $(J_f,T_f,\Delta T)=(\frac{9}{2},\frac{1}{2},0)$, $(\frac{9}{2},\frac{1}{2},1)$, $(\frac{7}{2},\frac{1}{2},0)$, $(\frac{7}{2},\frac{1}{2},1)$, $(\frac{9}{2},\frac{3}{2},1)$, and $(\frac{7}{2},\frac{3}{2},1)$, $Z^2=0.511$, 0.195, 0.413, 0.142, 0.315, and 0.271, respectively.

IV. RESULTS

A. Comparison with other carbon isotopes

Figure 1 shows energy spectra for electrons scattered through 180° from ^{12}C, ^{13}C, and ^{14}C. Each spectrum was measured at a momentum transfer close to the predicted maximum of the $M4$ form factor. As has been observed in other reactions, candidates for strong $M4$ excitations in ^{13}C appear at 9.50±0.01 MeV, 16.08±0.01 MeV ($\Gamma=148\pm13$ keV), and 21.47±0.01 MeV ($\Gamma=268\pm14$

TABLE II. Wave functions for $\frac{7}{2}^+$ and $\frac{9}{2}^+$ states in the weak coupling representation.

$J^+;T$	E_x (MeV)	Weak coupling components[a]		
$\frac{9}{2}_1;\frac{1}{2}$	9.45	$0.955(2_1;0)\otimes\frac{5}{2}$	$-0.203(4_1;0)\otimes\frac{5}{2}$	
$\frac{9}{2}_2;\frac{1}{2}$	15.46	$0.615(4_1;0)\otimes\frac{5}{2}$	$+0.570(4_1;0)\otimes\frac{1}{2}$	$+0.313(2_1;1)\otimes\frac{5}{2}$
		$-0.279(3_1;1)\otimes\frac{5}{2}$		
$\frac{9}{2}_3;\frac{1}{2}$	16.88	$0.198(4_1;0)\otimes\frac{3}{2}$	$-0.641(4_1;0)\otimes\frac{1}{2}$	$+0.495(2_1;1)\otimes\frac{5}{2}$
		$-0.322(3_1;1)\otimes\frac{5}{2}$		
$\frac{7}{2}_4;\frac{1}{2}$	15.90	$0.519(1_1;0)\otimes\frac{5}{2}$	$-0.617(1_1;1)\otimes\frac{5}{2}$	$-0.333(2_1;1)\otimes\frac{5}{2}$
$\frac{7}{2}_5;\frac{1}{2}$	16.13	$0.514(1_1;0)\otimes\frac{5}{2}$	$+0.277(2_1;0)\otimes\frac{5}{2}$	$+0.285(4_1;0)\otimes\frac{1}{2}$
		$+0.322(2_1;1)\otimes\frac{5}{2}$	$-0.211(2_2;1)\otimes\frac{3}{2}$	$-0.228(2_2;1)\otimes\frac{5}{2}$
$\frac{9}{2}_1;\frac{3}{2}$	21.48	$0.932(2_1;1)\otimes\frac{5}{2}$	$+0.235(3_1;1)\otimes\frac{3}{2}$	
$\frac{7}{2}_1;\frac{3}{2}$	20.69	$-0.648(1_1;1)\otimes\frac{5}{2}$	$+0.662(2_1;1)\otimes\frac{5}{2}$	
$\frac{7}{2}_2;\frac{3}{2}$	22.01	$0.614(1_1;1)\otimes\frac{5}{2}$	$+0.484(2_1;1)\otimes\frac{5}{2}$	$-0.383(2_2;1)\otimes\frac{5}{2}$
		$+0.385(3_1;1)\otimes\frac{5}{2}$		

[a]The energies of the physical core states are 4.44, 12.71, 14.08, 15.11, 16.11, 18.80, and 20.5 MeV for $(J;T)=(2_1;0)$, $(1_1;0)$, $(4_1;0)$, $(1_1;1)$, $(2_1;1)$, $(2_2;1)$, and $(3_1;1)$, respectively.

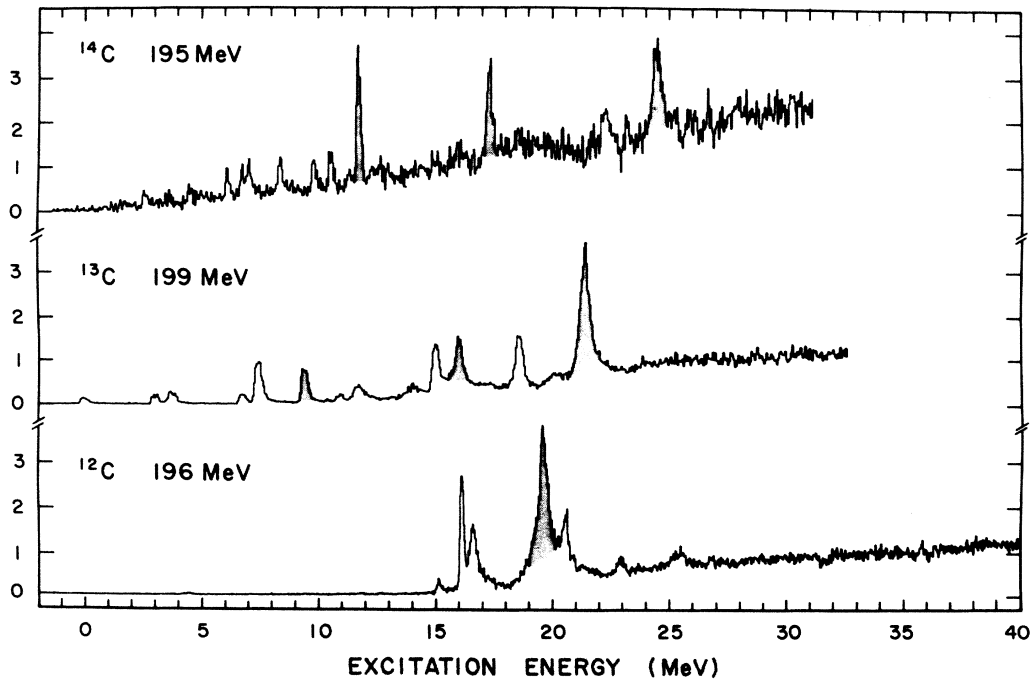

FIG. 1. Spectra of electrons scattered through 180° from carbon isotopes. Each spectrum was measured at a momentum transfer where $M4$ excitations have approximately the maximum cross section.

keV). Although the form factors for these peaks display the broad q dependence expected of an $M4$ transition, unambiguous multipole assignments cannot be made solely on the basis of form factor shape: Lower multipole transitions to configuration-mixed states can have similarly broad form factor q dependences.[21] The $M4$ assignments may be consolidated by comparing the three carbon spectra with the results of detailed shell model calculations. These results are depicted in Fig. 2. Backward-angle electron scattering is primarily a probe of isovector transitions so that the (e,e') cross sections vary approximately as Z_1^2. Since (π,π') and (p,p') are inherently more sensitive to isoscalar transitions, one can expect, on the basis of Fig. 2, quantitative differences with the relative cross sections measured in (e,e'). As Kurath and Lee[18] have emphasized, although there exists some correlation between the various reactions, the prominent peaks observed in (e,e') are not necessarily due to the same states accessed in either (π,π') or (p,p').

The simplest $M4$ spectrum is expected for the self-conjugate nucleus ^{12}C, where the shell model[21] predicts strong $\Delta T=0$ and $\Delta T=1$ $M4$ transitions to two states near 18.4 MeV. These transitions have been identified as major components of a peak observed in various reactions at 19.5 MeV. The comparison of $(\pi^+,\pi^{+\prime})$ and $(\pi^-,\pi^{-\prime})$ cross sections[22] revealed that these two states are isospin mixed. The 19.5 MeV peak is also known to include excitations not of $M4$ character.[21] Other sizable peaks in the ^{12}C spectrum have been attributed to lower multipole electric and magnetic transitions.[21]

In (π,π') measurements on ^{14}C, three candidate 4^- states were observed[20,23] at 11.7, 15.2, and 17.3 MeV. Al-

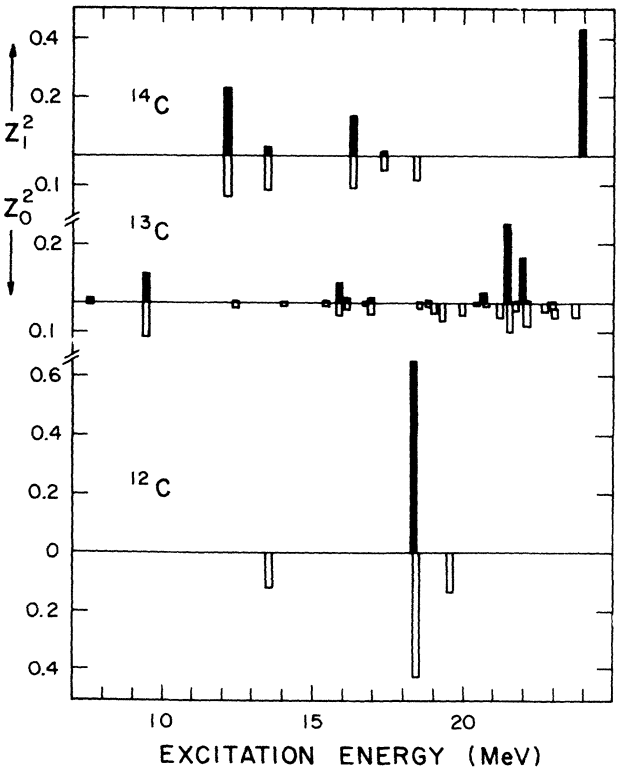

FIG. 2. Squared shell model transition amplitudes obtained for $M4$ excitations in carbon isotopes. Isovector amplitudes are represented by solid bars and read upward. Isoscalar amplitudes are represented by open bars and read downward.

though the 11.7 and 17.3 MeV levels were also apparent in (e,e') measurements,[17] the 15.2 MeV level was not. On the other hand, the electron experiment revealed an additional 4^- candidate not seen in the (π,π') work, at 24.3 MeV. These observations are consistent with the shell model predictions represented in Fig. 2. The levels observed in both reactions, at 11.7 and 17.3 MeV, are identified with theoretical $4^-;T=1$ states at 12.1 and 16.3 MeV, for which the model predicts large isoscalar and isovector transition amplitudes. The 15.2 MeV level is associated with a $4^-;T=1$ state calculated at 13.5 MeV. In this case the model gives only small isovector strength so that the contribution in an (e,e') spectrum should be weak. Finally, the peak appearing in the electron measurements at 24.3 MeV corresponds to a predicted $T=2$ state, not accessible through the isoscalar operator which plays the dominant role in (π,π') reactions.

The shell model predicts a more fragmented $M4$ spectrum for ^{13}C. Of the candidate $M4$ peaks in the (e,e') spectrum, only that at 9.50 MeV may be uniquely associated with a single theoretical level, a $\frac{9}{2}^+;T=\frac{1}{2}$ state. As noted previously, in the vicinities of the two other $M4$ candidates, at 16.08 and 21.47 MeV, the shell model indicates not one, but several $M4$ excitations. Table I shows that the largest contribution to the 16.08 MeV peak is expected to come from a $\frac{7}{2}^+;T=\frac{1}{2}$ state, whereas two $T=\frac{3}{2}$ states, one $\frac{9}{2}^+$ and the other $\frac{7}{2}^+$, have been predicted to provide most of the cross section for the 21.47 MeV peak. As in the case of ^{14}C, pion scattering measurements show a possible fourth $M4$ peak,[4] not apparent in the (e,e') data. The energy of this peak, 17.9 MeV, suggests identification with a cluster of isoscalar $M4$ transitions predicted near 19 MeV.

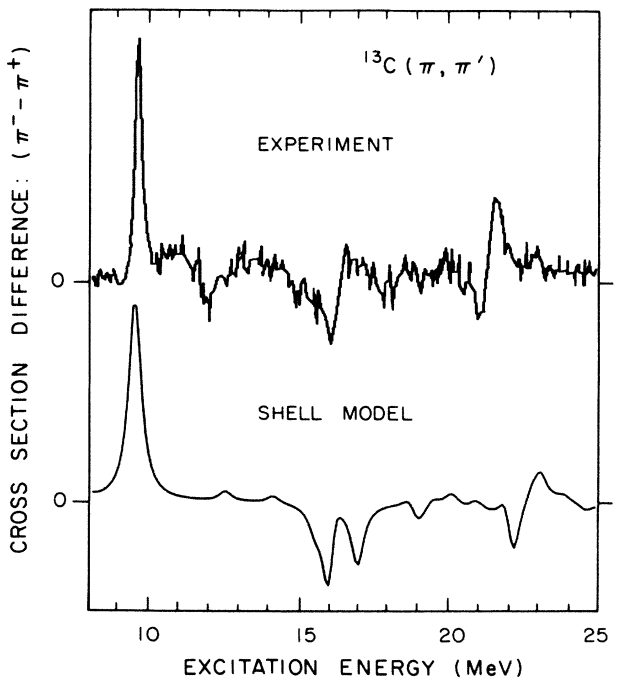

FIG. 3. Cross section difference for the inelastic scattering of 162 MeV π^- and π^+ particles from ^{13}C. The shell model curve, for $M4$ transitions only, has been smeared with a Lorentzian function of width 0.5 MeV. The ordinate scales are in arbitrary units.

More detailed information on the isospin character of the $M4$ transitions is obtained from the difference between $(\pi^-,\pi^{-'})$ and $(\pi^+,\pi^{+'})$ cross sections.[2] For incident pion kinetic energies close to 162 MeV, $(\pi^-,\pi^{-'})$ cross sections are about nine times larger for a pure neutron excitation than $(\pi^+,\pi^{+'})$ cross sections. The opposite applies for pure proton excitations. Thus the 9.50 MeV transition, which has a $(\pi^-,\pi^{-'})$ cross section eleven times larger than the (π^+,π^+) cross section,[4] would appear to be a rather pure neutron transition. As shown in Fig. 3, the 16.08 MeV peak is larger in $(\pi^+,\pi^{+'})$, and is therefore identified as a proton excitation. The structure in the cross section difference near 21.5 MeV attests to the existence of $T=\frac{1}{2}$ levels in this region, since pure $T=\frac{3}{2}$ states are excited only by the isovector operator which gives neutron and proton amplitudes of equal magnitude. It has not yet been established whether the $T=\frac{1}{2}$ states are isospin mixed with $T=\frac{3}{2}$ states, similar to the mixing which occurs in ^{12}C. Based on the shell model results presented in Table I, the opportunity for considerable mixing is present. For both $J^\pi=\frac{9}{2}^+$ and $\frac{7}{2}^+$, calculated $T=\frac{1}{2}$ and $T=\frac{3}{2}$ states are found nearly degenerate in energy.

Figure 3 also shows the shell model prediction for the difference between the π^- and π^+ cross sections at the peak of the $M4$ angular distribution[18] $\sigma^- - \sigma^+ = 792 Z_0 Z_1$ (μb/sr). The calculation correctly describes most of the features seen in the measured cross section difference. One exception is that the π^+ excess cross section predicted near 16 MeV is too fragmented in comparison with the data. Unaccounted for asymmetry at 12 MeV may be due to $E3$ excitations not included in the calculation. Otherwise the shell model result is in remarkably good agreement with the data, even reproducing such details as the bipolar structure at 22 MeV and the small π^+ excess near 18 MeV.

To summarize, it has been shown how shell model calculations lie in good accord with the excitation energies of proposed $M4$ transitions in three carbon isotopes, ^{12}C, ^{13}C, and ^{14}C. Moreover, the model appears to describe not only the relative cross sections of these transitions, but also gives a good account of their isospin character. Thus, even though the observed q dependence of these transitions is not by itself a conclusive signature of $M4$ excitation, the systematic and multifaceted agreement between experiment and theory makes such an assignment seem assured.

B. Electron scattering form factors

Transverse form factors for the three $M4$ peaks in ^{13}C are shown in Fig. 4. *A priori*, one might expect continuum effects to influence these form factors differently. Whereas the $d_{5/2}$ neutron excited in the 9.50 MeV transition is unbound by 0.11 MeV with respect to the 4.44 MeV 2^+ parent in ^{12}C, the 16.08 MeV proton transition lies 1.45 MeV below the proton separation energy. The 21.47 MeV peak is unbound for both neutrons and pro-

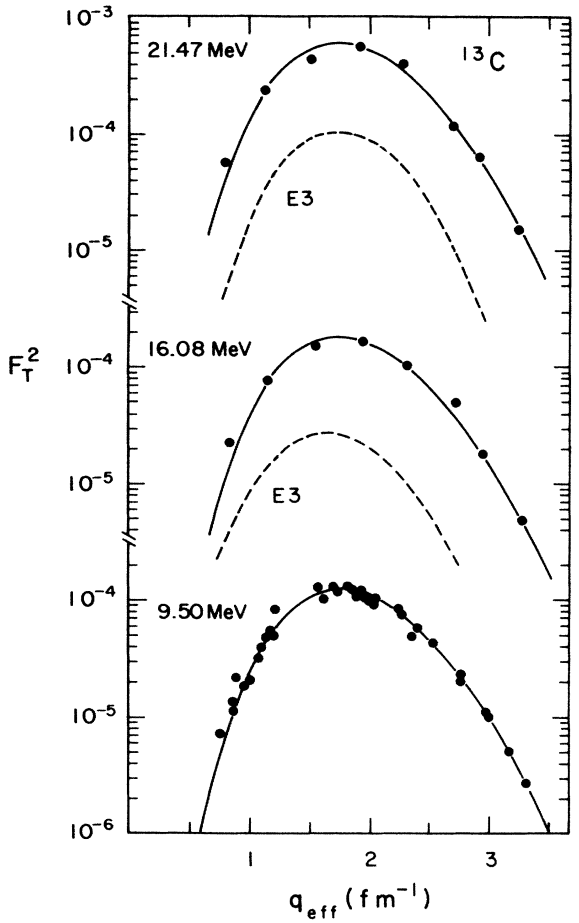

FIG. 4. Transverse (e,e') form factors for $M4$ excitations in ^{13}C. The continuous curve, a phenomenological $M4$ fit to the 9.50 MeV form factor, also describes the shape of the 16.08 and 21.47 MeV form factors. The dashed curves show the results of shell-model calculations for $E3$ transitions to levels in the vicinity of 16.08 and 21.47 MeV. Corrections for nucleon finite size and shell-model center-of-mass effects are included in the calculations. The effective momentum transfer q_{eff}, defined in Ref. 21, contains lowest-order corrections for Coulomb distortion of the incoming and outgoing waves.

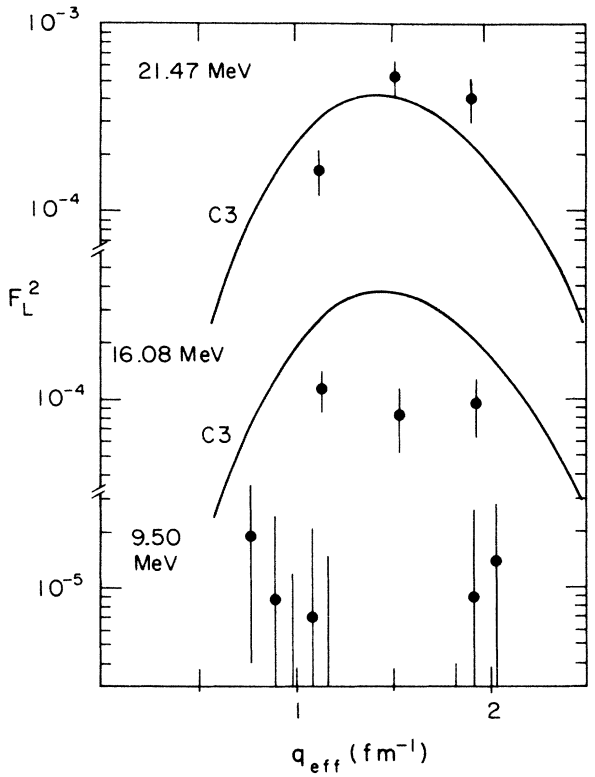

FIG. 5. Longitudinal form factors for predominantly $M4$ peaks in ^{13}C. The curves show the results of shell model calculations for $C3$ transitions to levels in the vicinity of 16.08 and 21.47 MeV.

tons. Nevertheless, the phenomenological $M4$ curve fitted to the 9.50 MeV data also gives a good description of the 16.08 and 21.47 MeV form factors. Thus these results give no clear evidence for continuum modifications to the final state wave functions.

Another point of concern for ^{13}C is that the same $\frac{7}{2}^+$ and $\frac{9}{2}^+$ levels excited by the $M4$ operator may also be reached by $E3$ and $E5$ transitions. Unlike the $M4$ multipole, the $E3$ and $E5$ transition operators have associated longitudinal $C3$ and $C5$ form factors. Consequently, the existence of finite longitudinal form factors F_L^2 for the peaks of interest confirms that $E3$ or $E5$ contributions must be present in the transverse form factors. Figure 5 shows F_L^2 derived from Rosenbluth comparisons of cross sections measured at the same momentum transfers, but different scattering angles. The results obtained for the 9.50 MeV peak set an upper limit of about 10^{-5} on F_L^2. Indeed, the probability of $E5$ excitation of the $\frac{9}{2}^+$ level is expected to be weak since, unlike the $E3$ multipole, it involves highly-excited configurations, outside the configuration space of the present calculations. A longitudinal form factor consistent with zero identifies the transition as being either magnetic, a pure neutron excitation, or both.

In Fig. 6, the transverse form factor determined for the transition to the 9.50 MeV state is compared to the results of two plane-wave Born approximation calculations for the single-particle $(d_{5/2},p_{3/2}^{-1})_{M4}$ matrix element. Each of these calculations employed two free parameters which were fitted to the data: an overall normalization factor, and a size parameter for the radial wave functions. The harmonic oscillator calculation shown in Fig. 6 is for an oscillator size of $b=1.53$ fm, and has a magnitude equal to 0.052 ± 0.001 of the extreme single-particle limit for the $(d_{5/2},p_{3/2}^{-1})_{M4,\Delta T=1}$ matrix element,[21] corresponding to $Z_1^2=1$.

The contribution of two-body meson-exchange currents, recently evaluated by Plum *et al.*,[17] is expected to uniformly increase the one-body form factor by about 20%. As has been noted by Bergstrom, Neuhausen, and Lahm,[24] a better fit to the form factor shape is obtained when the analysis is repeated with Woods-Saxon wave functions.

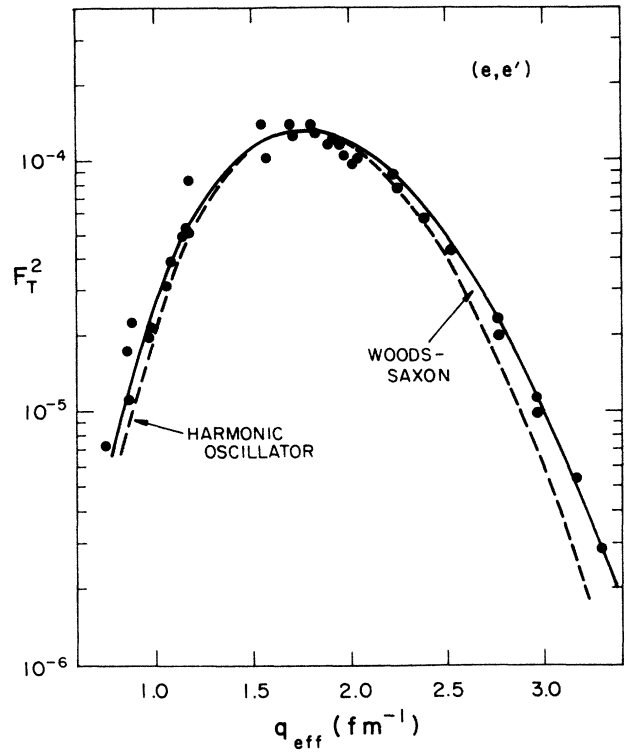

FIG. 6. Transverse form factor for the 9.50 MeV excitation in ^{13}C and comparison with $(1d_{5/2}, 1p_{3/2}^{-1})_{M4}$ fits using harmonic oscillator and Woods-Saxon wave functions.

For this calculation in the relative coordinate frame,[25] the relevant single-neutron energies were set to $E(1p_{3/2}) = -10$ MeV and $E(1d_{5/2}) = -1$ MeV in a potential well of diffuseness 0.50 fm and radius $1.15(A-1)^{1/3}$ fm. In comparison with the harmonic oscillator calculations, the use of Woods-Saxon wave functions decreases the predicted form factor by 23%, thereby canceling the enhancement brought about by exchange currents. Consequently, the net result of considering exchange currents and Woods-Saxon wave functions is a corrected one-body transition strength equal to 0.053 ± 0.001 of the isovector single-particle limit, close to the original value obtained in the unembellished oscillator analysis.

The 16.08 and 21.47 MeV peaks, which are predicted to include strongly excited $\frac{7}{2}^+$ levels, have considerably larger longitudinal form factors than the 9.50 MeV transition. The curves shown in Fig. 5 represent the sums of $C3$ form factors calculated without effective charges for theoretical $\frac{5}{2}^+$ and $\frac{7}{2}^+$ states in the excitation energy ranges 15.65–16.80 MeV and 20.48–22.01 MeV. The corresponding model predictions for the transverse form factors F_T^2, shown in Fig. 4, give $E3$ components which amount to only $\sim 15\%$ corrections to the measured data. The conclusions that can be drawn from these comparisons are only crudely quantitative. Although the restricted-basis shell model usually gives reliable predictions of form factor shapes, the calculated magnitudes are commonly in error by factors of 2 or more. Neglected core polarization effects strongly modify the magnitude of (e,e') form factors, increasing F_L^2 and reducing F_T^2. For example, the transverse form factor for the 20.6 MeV level in ^{12}C, considered to be a $3^-;T=1$ state, is at least a factor of 3 smaller than the $E3$ form factor given by the shell model.[21] In light of these observations, the $E3$ multipole was assumed to make a 5 ± 5 % contribution in both the 16.08 and 21.47 MeV peaks. As will be discussed later, small $E3$ contributions are also consistent with (π,π') excitation functions measured at a momentum transfer close to the maximum of the $M4$ angular distributions.[3]

After applying the estimated corrections for the $E3$ multipole, the $M4$ transition strengths in the 16.08 and 21.47 MeV peaks were determined, again in terms of the isovector single-particle limit.[21] The results, given in Table III, are remarkably consistent with those obtained for ^{12}C and ^{14}C. In each case, the total $M4$ cross section measured in (e,e') amounts to roughly 35% of the isovector single-particle limit. In comparison with the shell model, only about half the predicted strength is observed.

Another interesting consistency is found in the harmonic oscillator size parameters deduced by fitting the $M4$ form factors in the three carbon isotopes: 1.52 ± 0.02, 1.53 ± 0.01, and 1.52 ± 0.04 fm, in order of increasing mass. These values lie about 7% below the 1.65 fm that is obtained from the ground state charge radius which represents an average over all occupied proton orbits. Since it is assumed that the q dependence of the $M4$ form factor depends almost exclusively on the radial wave functions of the $1p_{3/2}$ and $1d_{5/2}$ orbits, this result indicates that one (or perhaps both) of these orbits has a smaller size than would be expected on the basis of the average oscillator radius parameter. Recent electron scattering measurements[26] of $M3$ transitions in ^{10}B are consistent with $b = 1.47 \pm 0.02$ fm for the $1p_{3/2}$ orbit. Since the rms ground state charge radius of ^{10}B is close to that of the carbon isotopes,[27] this value should also be indicative of the $1p_{3/2}$ size in carbon. To the extent that the harmonic oscillator is a reasonable representation of the single-particle orbits in $1p$-shell nuclei, a small $p_{3/2}$ orbit size would in large part account for the small size parameter required to fit the $M4$ form factor.

C. Determination of transition amplitudes using (π,π'), (e,e'), and (p,p') data

Further insight into the properties of the 9.50 MeV transition can be derived from inelastic pion scattering and other reactions. In the fixed-scatterer, impulse approximation, the differential (π,π') cross sections have the form[28]

$$\sigma(q,\theta) \sim 4\mathcal{M}^2(q)\cos^2\theta + \mathcal{S}^2(q)\sin^2\theta ,$$

if the reaction is assumed to proceed through an intermediate $N^*(3,3)$ resonance. Both the spin-flip ($\mathcal{S}$) and spin-independent ($\mathcal{M}$) form factors contribute to electric transitions, although $\mathcal{M}(q)$ is usually more important. For magnetic transitions only $\mathcal{S}(q)$ contributes. Measurements[3] at constant momentum transfer q, near the max-

TABLE III. Comparison of (e,e') $M4$ cross sections in carbon isotopes. The experimental and shell model cross sections σ_{expt} and σ_{SM} are measured in units of the isovector single-particle limit (Ref. 21) corresponding to $Z_1=1$, $Z_0=0$, and are corrected for one-pion exchange current contributions. Woods-Saxon wave functions are assumed. Results for ^{12}C and ^{14}C are from Refs. 21 and 17. The experimental cross section given for the 24.4 MeV transition in ^{14}C represents the average of two extreme fits to the data, with the assigned error encompassing both limits.

	E_x (MeV)	σ_{expt}	σ_{SM}	$\sigma_{expt}/\sigma_{SM}$
^{12}C	19.59	0.34±0.04	0.651	0.51±0.06
^{13}C	9.50	0.053±0.001	0.064	0.83±0.02
	16.08	0.072±0.008	0.165	0.44±0.05
	21.47	0.24±0.02	0.468	0.51±0.04
		0.36±0.02	0.697	0.52±0.03
^{14}C	11.7	0.09±0.03	0.167	0.53±0.18
	17.3	0.11±0.03	0.188	0.59±0.16
	24.4	0.19±0.06	0.435	0.42±0.14
		0.39±0.07	0.790	0.49±0.09

imum cross section for the 9.50 MeV transition, show the $\sin^2\theta$ dependence expected of a magnetic transition, and thus support the neglect of the $E5$ multipole in the interpretation of the (e,e') data.

Under the assumption that the stretched $(d_{5/2},p_{3/2}^{-1})_{M4}$ matrix element dominates, the spin-flip form factor $\mathcal{S}(q)$ is given by

$$\mathcal{S}(q)=Z_1G_1\rho^s_{M4}(q)+Z_0G_0\rho^s_{M4}(q)\ ,$$

where ρ^s_{M4} is the one-body spin transition density

$$\rho^s_{M4}(q)=\langle d_{5/2}||j_3(qr)[Y_3(r)\times\sigma]_4||p_{3/2}\rangle\ ,$$

and the parameters G_0 and G_1 are proportional to the pion-nucleon scattering amplitudes. In the vicinity of the $N^*(3,3)$ resonance, G_0 and G_1 are related[28] by $G_0^-/G_1^-\cong 2$, $G_0^+/G_1^+\cong -2$, and $|G_0^-/G_0^+|\cong 1$, where the $+$ and $-$ superscripts indicate π^+ and π^- inelastic scattering. Dehnhard *et al.*[2] have expressed the differences between π^+ and π^- cross sections in terms of the asymmetry parameter.

$$A_\pi=\frac{\sigma^- -\sigma^+}{\sigma^- +\sigma^+}=\frac{Z_1/Z_0}{1+(Z_1/2Z_0)^2}\ .$$

For the 9.5 MeV transition in ^{13}C a marked asymmetry is observed,[4] $A_\pi=0.83\pm0.10$, corresponding to $\sigma^-:\sigma^+=11:1$. Two possible solutions emerge for the isovector-to-isoscalar transition amplitude ratio,

$$Z_1/Z_0=1.07\pm0.25 \text{ or } 3.7\pm0.6\ .$$

If the transition is represented by neutron and proton amplitudes, $Z_n=(Z_0+Z_1)/\sqrt{2}$ and $Z_p=(Z_0-Z_1)/\sqrt{2}$, the first solution is seen to be for an almost pure neutron excitation. The second solution is for a dominantly isovector transition. The existence of two possible solutions, previously noted by Rikus *et al.*,[5] demonstrates that simple ratios of π^- and π^+ cross sections alone are insufficient to uniquely define the isospin character of a particular transition.

In order to isolate the correct solution, Peterson *et al.*[10] have measured the ratio of the (^{3}He,t) and (^{3}He,^{3}He') cross sections. Whereas the charge-exchange reaction is purely isovector, inelastic scattering is more sensitive to the isoscalar excitations. A quantitative analysis[10] of the ^{3}He cross section ratio gave $Z_1/Z_0=-4.2$ or 0.72. Although the reliability of such treatments has yet to be established, only the second solution is reasonably consistent with the (π,π') ratio.

The magnitudes of Z_0 and Z_1 can be fixed by the measured (e,e') cross section which may be written

$$\sigma^e\sim[Z_1\mu_1\rho^s_{M4}(q)+Z_0\mu_0\rho^s_{M4}(q)]^2\ ,$$

where $\mu_1=-2.353\ \mu_N$ and $\mu_0=0.440\ \mu_N$ are the isovector and isoscalar magnetic moments. From the Woods-Saxon analysis presented above we have

$$\frac{\sigma^e}{\sigma_1^e}=\left[Z_1+\frac{\mu_0}{\mu_1}Z_0\right]^2=(Z_1-0.187Z_0)^2=0.053\pm0.001\ ,$$

where σ_1^e represents the maximum possible isovector cross section ($Z_1=1$, $Z_0=0$). Combining this relationship with the (π,π') result $Z_1/Z_0=1.07\pm0.25$ yields $Z_1=0.28\pm0.02$ and $Z_0=0.26\pm0.07$. These values are about 20% lower than the transition amplitudes given by the shell model, $Z_1=0.330$ and $Z_0=0.342$. Although Z_1 is well determined, by virtue of the dominant isovector sensitivity of electron scattering, the value established for

Z_0 is less precise. Further information on Z_0 may be sought from the absolute (π,π') and (p,p') cross sections which are more sensitive to isoscalar transitions: Since $|G_0/G_1| \simeq 2$, the (π,π') cross section for a purely isoscalar transition will be approximately four times larger than that for a pure isovector transition of the same intrinsic strength. Moreover, for the 135 MeV kinematics of the (p,p') data,[5,6] isoscalar $M4$ cross sections are favored over isovector $M4$ by a factor of about 2.

Although the (π,π') and (p,p') reactions are not as well understood as electron scattering, in recent years considerable effort has been devoted to improving the effective interactions used in their analysis. In the case of inelastic pion scattering, unnatural-parity levels are excited only through the spin-orbit part of the pion-nucleon interaction. Carr *et al.*,[29] for example, have constructed the effective pion-nucleus interaction by folding the p-wave form of the pion-nucleon spin operator with the initial and final state wave functions of the target nucleus. The effective nucleon-nucleon interaction in (p,p') is more involved since one must not only consider spin-orbit, tensor, and central interactions, but also the possibility of knockout exchange. For (p,p') with proton energies in the range 10—200 MeV, recent theoretical studies have indicated that only the central components of the nucleon-nucleon interaction are appreciably modified by effects due to the nuclear medium.[30] A review of the current status of (π,π') and (p,p') cross section calculations has been given by Petrovich and Love.[31]

In the present work, the (π,π') and (p,p') cross sections were evaluated using the general inelastic scattering program ALLWRLD (Ref. 32) which generates reduced transition potentials for the distorted-wave, impulse approximation codes MSUDWPI (Ref. 33) and RAMUT (Ref. 34). The (π,π') formalism in MSUDWPI does not assert isobar dominance, as sketched above, but defines a more general form for the spin-orbit operator in the effective interaction.[33] The pion-nucleus optical potential of Carr[29] was used. Inelastic proton scattering cross sections were computed with the 135 MeV Love-Franey effective interaction[35] and the "best" ^{13}C optical model parameter set of Collins *et al.*[36] The Woods-Saxon transition density preferred by the (e,e') results was employed with approximate center-of-mass corrections based on the harmonic oscillator formalism.

Calculations were performed for different values of the transition amplitudes Z_0 and Z_1, using as a starting point the values established above, $Z_1=0.28$ and $Z_0=0.26$. For these values, the calculated (p,p') cross sections were in excellent agreement with the 135 MeV data of Rikus *et al.*[5] However, the $(\pi^-,\pi^{-'})$ calculations were about 20% below the cross sections[2] measured with 162 MeV pions. A somewhat better compromise, shown in Fig. 7, was obtained by increasing Z_0 slightly to 0.27. A change of this small magnitude in Z_0 does not affect the good agreement obtained for the Woods-Saxon fit to the (e,e') form factor represented in Fig. 6.

A final test of the deduced transition amplitudes is provided by the measured (π,π') excitation function,[3] shown in Fig. 8. In this case the $(\pi^-,\pi^{-'})$ cross sections were obtained at constant momentum transfer, close to the maximum of the $M4$ angular distribution. The calculated excitation function is seen to give a good description of the data over a wide range of pion energies, decreasing with increasing pion kinetic energy (or decreasing $\sin^2\theta$), as expected for a magnetic transition.

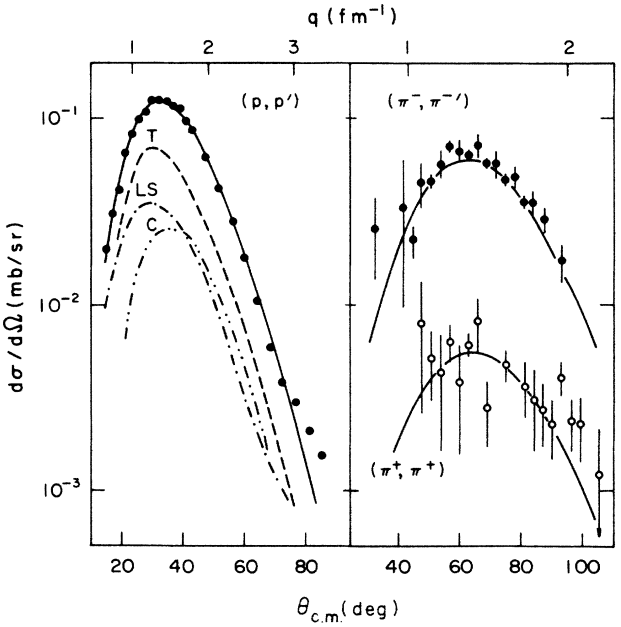

FIG. 7. Inelastic (p,p') and (π,π') cross sections (Refs. 2 and 5) for excitation of the 9.50 MeV level in ^{13}C. The incident kinetic energies were 135 MeV for protons, and 162 MeV for pions. The curves were evaluated in the distorted-wave impulse approximation using the same Woods-Saxon wave functions that fit the (e,e') form factors. The calculations were for isoscalar and isovector transition amplitudes $Z_0=0.27$ and $Z_1=0.28$, and no further normalization was applied. Tensor, central, and spin-orbit components in the calculated (p,p') cross section are indicated separately.

Considering that Z_0 and Z_1 are the only structure amplitudes employed in the combined analysis, it is remarkable that the absolute magnitudes of the (e,e'), (p,p'), $(\pi^-,\pi^{-'})$, and $(\pi^+,\pi^{+'})$ cross sections can be so accurately reproduced. Moreover, the q dependence of the $M4$ transition density $\rho^s_{M4}(q)$, which was fitted to the (e,e') data, also gives a good account of the (p,p') and (π,π') angular distributions.

In a similar combined analysis of $M6$ and $M4$ transitions in ^{28}Si and ^{16}O, Carr *et al.*[29] calculated $(\pi^+,\pi^{+'})$ and $(\pi^-,\pi^{-'})$ cross sections that were, respectively, 15% and 30% larger than the experimental data. This was interpreted as evidence that the strength of the spin-orbit component in the pion-nucleus effective interaction should be raised by 7—15%. Subsequent analyses[20,37] of ^{14}C and ^{14}N suggested raising the spin-orbit strength by 20—40%. Although the present analysis would be improved by a small increase in the calculated (π,π') cross section, the required change in the spin-orbit strength parameter is less than 10%. We have refrained from making such modifications since there exist other reservations

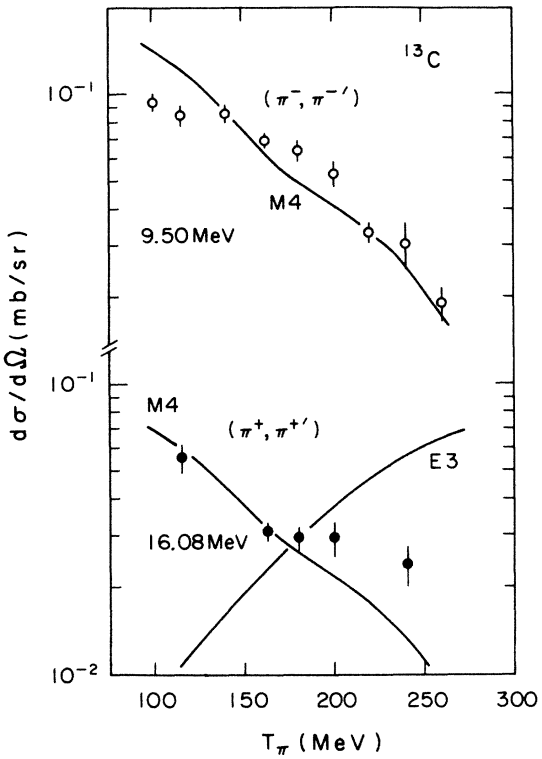

FIG. 8. Inelastic pion scattering excitation functions (Ref. 3) measured at constant momentum transfer for the 9.50 and 16.08 MeV excitations in ^{13}C. The theoretical curves were computed using the code MSUDWPI (Ref. 33), and correspond to transition amplitudes deduced in the text. The normalization of the $E3$ curve is arbitrary.

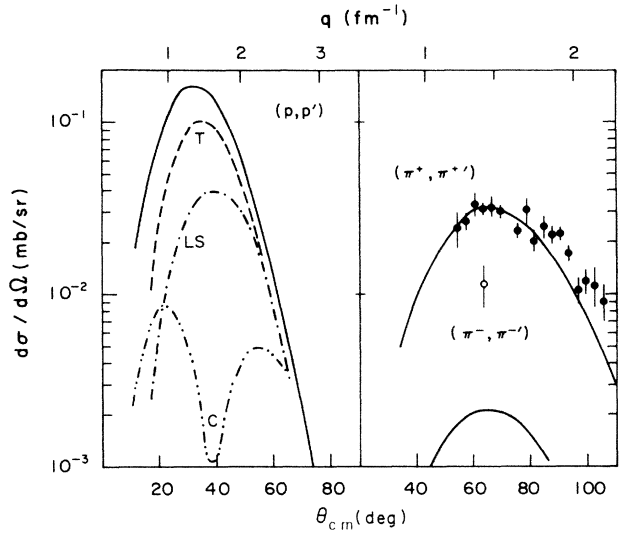

FIG. 9. Inelastic cross sections for the excitation of the 16.08 MeV level in ^{13}C by 135 MeV protons and 162 MeV pions. The curves are for isoscalar and isovector amplitudes $Z_0=-0.22$ and $Z_1=0.25$ and use the same Woods-Saxon wave functions that fit the (e,e') form factor.

which affect the interpretation of pion scattering. For example, Karapiperis and Moniz[38] have shown that the dominant reaction mechanism through an intermediate $N^*(3,3)$ resonance does not have a simple theoretical description because the isobar readily couples to the nuclear medium, and this interaction is strongly isospin dependent. A specific calculation[38] for $M4$ transitions in ^{16}O gave an $\sim 15\%$ correction to the relative isovector and isoscalar transition amplitudes. The interpretation of the (p,p') reaction is also subject to uncertainty. For example, when the calculations were repeated using an alternative optical potential, the resultant (p,p') cross sections were increased by about 10%. In addition, the code RAMUT (Ref. 34) contains approximations in the evaluation of the knockout exchange reaction, which also affect the calculated cross sections at the 10% level.

Under the assumption that the same single state is seen in both (e,e') and (π,π'), a similar analysis has been carried out for the 16.08 MeV peak. Inelastic proton scattering cross sections for this peak are not available, and only a single data point has been obtained with π^- mesons. A combined analysis of the (e,e') and $(\pi^+,\pi^{+\prime})$ data gives $Z_0=-0.22\pm0.04$ and $Z_1=0.25\pm0.03$, corresponding to $Z_p/Z_n\cong-15$. Thus the 16.08 MeV excitation is found to be a purer proton transition than suggested by a previous analysis, based on (π,π') ratios alone,[2] which gave $Z_p/Z_n=-1.3$ or $+3.0$. The reason for this is evident from Fig. 9, where the $(\pi^-,\pi^{-\prime})$ datum is seen to be about 3 standard deviations above the curve derived from (e,e') and $(\pi^+,\pi^{+\prime})$. In the $(\pi^-,\pi^{-\prime})$ spectrum,[2] the 16.08 MeV transition is obscured in a background of neighboring levels. Consequently, the π^- point is perhaps better regarded as an upper limit. As shown in Fig. 8, the measured (π,π') excitation function confirms that this transition is mainly of magnetic character, although a small $E3$ component is not ruled out. Near agreement of (p,p') measurements with the predicted cross sections would suggest that the same level was being observed in all reactions, and that the $M4$ transition strength is concentrated in a single level, rather than being fragmented, as predicted by the shell model.

V. CONCLUSIONS

By means of a combined analysis of (e,e'), (π,π'), and (p,p') data, isoscalar and isovector transition amplitudes were determined for $M4$ excitations in ^{13}C. In particular, the transition amplitudes deduced for the 9.50 MeV excitation give a remarkably consistent description of all existing measurements. By virtue of the dominant isovector sensitivity of the well-understood (e,e') reaction, the isovector amplitudes are precisely determined. The isoscalar transition amplitudes are less well known since these are derived primarily from (π,π') and (p,p') scattering, for which the present theoretical description is only approximate. Nevertheless, the overall level of agreement encourages further study of the usefulness of intermediate-energy (p,p') and (π,π') as quantitative probes of nuclear structure.

Consistency has also been shown to exist with $M4$ excitations in the other carbon isotopes, ^{12}C and ^{14}C. In each case detailed shell model calculations accurately give the energies, relative strengths, and isospin character of the observed $M4$ transitions. As discussed elsewhere,[39] the most striking failure of the shell model is that the predicted cross sections are systematically too large. For all three carbon isotopes, the shell model (e,e') cross sections exceed the data by a factor of 2. The origins of this "quenching" are not certain. One-pion exchange currents are not responsible, since calculations specifically show that these effects should increase the observed cross sections, not reduce them. Another suggestion, involving admixtures of isobar-hole configurations in the final states, was subsequently shown to have little consequence for magnetic transitions to "stretched" angular momentum levels,[40,41] particularly for nuclei as light as carbon. The favored explanation at present is the truncation of the shell model basis space. Expansion of the model space to include higher-excited configurations is expected to both reduce and fragment the predicted transition strength. In particular, it has been shown[21,42] that 2p-2h correlations in the ground state play a decisive role in quenching magnetic transition strengths. To investigate these effects in the shell model would require extremely large bases, even to extend by $2\hbar\omega$ the bases used in the present work. More phenomenological "core polarization" calculations have also been made,[42–46] but in general only for isolated transitions. A comprehensive and systematic study of core polarization effects on transitions of all multipoles, both magnetic and electric, has yet to be performed.

Another notable result of this study was the small radial size parameter required to describe the $M4$ cross sections, not only (e,e'), but also (π,π') and (p,p'). Recent (e,e') measurements in ^{10}B suggest a similarly small size parameter for $M3$ form factors, where the $1p_{3/2}$ orbit plays a leading role. Comparison of the three $M4$ form factors observed in ^{13}C showed no clear signature for continuum modifications in the final state wave functions.

ACKNOWLEDGMENTS

Dr. R. L. Huffman and Dr. B. Parker are thanked for assisting with this experiment. In addition, we are indebted to Dr. F. Petrovich, Dr. J. A. Carr, Dr. J. Kelly, and Dr. D. Halderson for supplying us with copies of their computer codes. This study was supported by the U.S. Department of Energy (Contract DE-AC02-76ER02853.A013) and by the National Science Foundation (Grant PHY-8217076).

---

*Present address: Department of Physics and Astronomy, University of Virginia, Charlottesville, VA 22901.

†Present address: Los Alamos National Laboratory, Los Alamos, NM 87545.

[1]R. A. Lindgren, W. J. Gerace, A. D. Bacher, W. G. Love, and F. Petrovich, Phys. Rev. Lett. **42**, 1524 (1979).

[2]D. Dehnhard, S. J. Tripp, M. A. Franey, G. S. Kyle, C. L. Morris, R. L. Boudrie, J. Piffaretti, and H. A. Thiessen, Phys. Rev. Lett. **43**, 1091 (1979).

[3]S. J. Seestrom-Morris, D. Dehnhard, D. B. Holtkamp, and C. L. Morris, Phys. Rev. Lett. **46**, 1447 (1981).

[4]S. J. Seestrom-Morris, D. Dehnhard, M. A. Franey, G. S. Kyle, C. L. Morris, R. L. Boudrie, J. Piffaretti, and H. A. Thiessen, Phys. Rev. C **26**, 594 (1982).

[5]L. Rikus, S. F. Collins, K. A. Amos, B. M. Spicer, G. G. Shute, I. Morrison, V. C. Officer, R. Smith, D. W. Devins, D. L. Friesel, and W. P. Jones, Aust. J. Phys. **35**, 9 (1982).

[6]S. F. Collins, G. G. Shute, B. M. Spicer, V. C. Officer, I. Morrison, K. A. Amos, D. W. Devins, D. L. Friesel, and W. P. Jones, Nucl. Phys. **A380**, 445 (1982).

[7]S. J. Seestrom-Morris, M. A. Franey, D. Dehnhard, D. B. Holtkamp, R. L. Boudrie, J. F. Amann, G. C. Idzorek, and C. A. Goulding, Phys. Rev. C **30**, 270 (1984).

[8]K. Min, E. J. Winhold, K. Shoda, M. Yamazaki, M. Torikoshi, H. Tsubota, and B. N. Sung, Phys. Rev. C **28**, 484 (1982).

[9]R. J. Peterson and J. J. Hamill, Phys. Rev. C **22**, 2282 (1980).

[10]R. J. Peterson, J. R. Shepard, and R. A. Emigh, Phys. Rev. C **24**, 826 (1981).

[11]W. Bertozzi, M. V. Hynes, C. P. Sargent, W. Turchinetz, and C. F. Williamson, Nucl. Instrum. **162**, 211 (1979).

[12]R. S. Hicks, A. Hotta, J. B. Flanz, and H. deVries, Phys. Rev. C **21**, 2177 (1980).

[13]See AIP document no. PAPS PRVC34-1161-4 for 4 pages of tabulated cross section measurements. Order by PAPS number and journal reference from American Institute of Physics, Physics Auxiliary Publication Service, 335 East 45th Street, New York, NY 10017. The price is $1.50 for each micorfiche or $5.00 for photocopies of up to 30 pages, and $0.15 for each additional page over 30 pages. Airmail additional. Make checks payable to American Institute of Physics.

[14]D. J. Millener and D. Kurath, Nucl. Phys. **A255**, 315 (1975).

[15]S. Cohen and D. Kurath, Nucl. Phys. **73**, 1 (1965).

[16]J. Raynal, Nucl. Phys. **A97**, 572 (1967).

[17]M. A. Plum, R. A. Lindgren, J. Dubach, R. S. Hicks, R. L. Huffman, B. Parker, G. A. Peterson, J. Lichtenstadt, M. A. Moinester, J. Alster, and H. Baer, Phys. Lett. **137B**, 15 (1984); M. A. Plum, private communication.

[18]T.-S.H. Lee and D. Kurath, Phys. Rev. C **22**, 1670 (1980).

[19]S. Cohen and D. Kurath, Nucl. Phys. **A101**, 1 (1967).

[20]D. B. Holtkamp, S. J. Seestrom-Morris, D. Dehnhard, H. W. Baer, C. L. Morris, S. J. Greene, C. J. Harvey, D. Kurath, and J. A. Carr, Phys. Rev. C **31**, 957 (1985).

[21]R. S. Hicks, J. B. Flanz, R. A. Lindgren, G. A. Peterson, L. W. Fagg, and D. J. Millener, Phys. Rev. C **30**, 1 (1984).

[22]C. L. Morris, J. Piffaretti, H. A. Thiessen, W. B. Cottingame, W. J. Braithwaite, R. J. Joseph, I. B. Moore, D. B. Holtkamp, C. J. Harvey, S. J. Greene, C. F. Moore, R. L. Boudrie, and R. J. Peterson, Phys. Lett. **86B**, 31 (1979).

[23]D. B. Holtkamp, S. J. Seestrom-Morris, S. Chakravarti, D. Dehnhard, H. W. Baer, C. L. Morris, S. J. Greene, and C. J. Harvey, Phys. Rev. Lett. **47**, 216 (1981).

[24]J. C. Bergstrom, R. Neuhausen, and G. Lahm, Phys. Rev. C **29**, 1168 (1984).

[25]D. J. Millener, J. W. Olness, E. K. Warburton, and S. S. Han-

na, Phys. Rev. C **28**, 497 (1983).
[26]R. S. Hicks *et al.* (unpublished).
[27]K. de Jager, H. de Vries, and C. de Vries, At. Data Nucl. Data Tables **14**, 479 (1974).
[28]E. R. Siciliano and G. E. Walker, Phys. Rev. C **23**, 2661 (1981).
[29]J. A. Carr, F. Petrovich, D. Halderson, D. B. Holtkamp, and W. B. Cottingame, Phys. Rev. C **27**, 1636 (1983).
[30]H. V. von Geramb, F. A. Brieva, and J. R. Rook, in *Microscopic Optical Potentials,* edited by H. V. von Geramb (Springer-Verlag, New York, 1979), Vol. 89, p. 104.
[31]F. Petrovich and W. G. Love, Nucl. Phys. **A354**, 499c (1981).
[32]J. A. Carr, F. Petrovich, D. Halderson, and J. Kelly, scattering potential code ALLWRLD (unpublished).
[33]J. A. Carr, distorted-wave code MSUDWPI (unpublished), adapted from the code DWPI, R. A. Eisenstein, and G. A. Miller, Comput. Phys. Commun. **11**, 95 (1976).
[34]F. Petrovich, private communication.
[35]W. G. Love and M. A. Franey, Phys. Rev. C **24**, 1073 (1981); W. G. Love, M. A. Franey, and F. Petrovich, in *Spin Excitations in Nuclei,* edited by F. Petrovich *et al.* (Plenum, New York, 1984).
[36]S. F. Collins, G. G. Shute, B. M. Spicer, V. C. Officer, I. Morrison, K. A. Amos, D. W. Devins, D. L. Friesel, and W. P. Jones, Nucl. Phys. **A380**, 445 (1982).
[37]D. F. Geesaman, as quoted in Ref. 20.
[38]T. Karapiperis and E. J. Moniz, Phys. Lett. **148B**, 253 (1984).
[39]R. A. Lindgren and F. Petrovich, in *Spin Excitations in Nuclei,* edited by F. Petrovich *et al.* (Plenum, New York, 1984); R. A. Lindgren, J. Phys. (Paris) **45**, C4 (1984).
[40]T. Suzuki, S. Krewald, and J. Speth, Phys. Lett. **107B**, 9 (1981).
[41]P. G. Blunden, B. Castel, and H. Toki, Z. Phys. A **312**, 247 (1983).
[42]S. Krewald and J. Speth, Phys. Rev. Lett. **45**, 417 (1980).
[43]T. Suzuki, H. Hyuga, A. Arima, and K. Yazaki, Phys. Lett. **106B**, 19 (1981); Nucl. Phys. **A358**, 421c (1981).
[44]J. Delorme, A. Figureau, and P. Guichon, Phys. Lett. **99B**, 187 (1981).
[45]P. G. Blunden and B. Castel, Phys. Lett. **135B**, 367 (1984); and private communication.
[46]B. Castel, I. P. Johnstone, and A. G. M. van Hees, Phys. Rev. C **32**, 323 (1985).

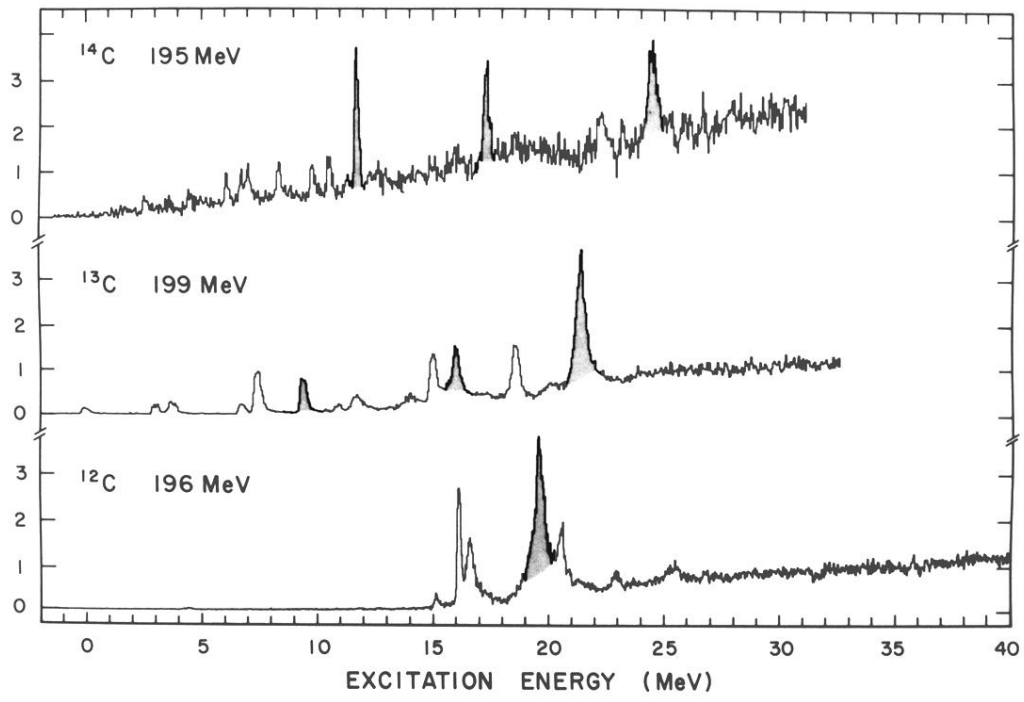

FIG. 1. Spectra of electrons scattered through 180° from carbon isotopes. Each spectrum was measured at a momentum transfer where $M4$ excitations have approximately the maximum cross section.